Imbalance of community structures in epilepsy

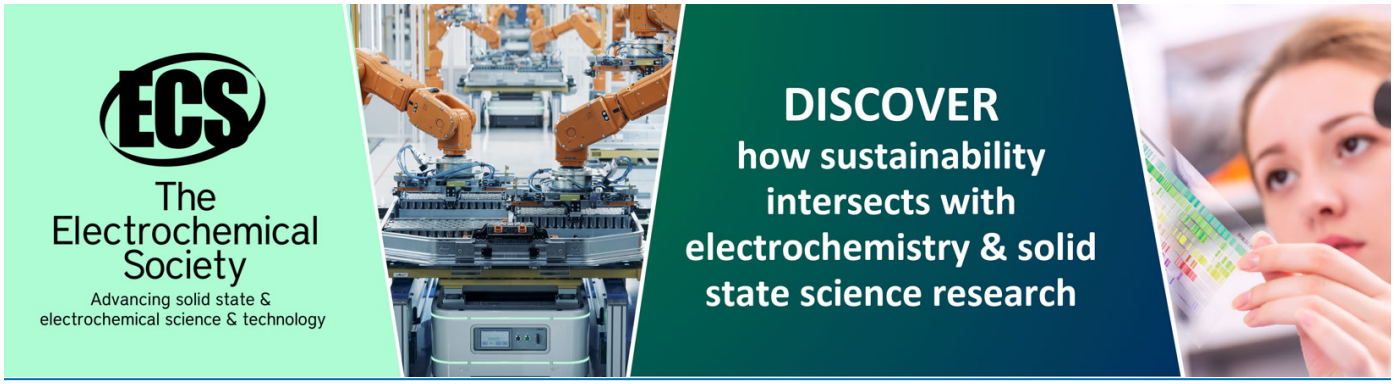

Journal of Physics: Conference Series **246** (2010) 012036 doi:10.1088/1742-6596/246/1/012036

Imbalance of community structures in epilepsy

Guillermo J. Ortega[1], Iván Herrera Peco[1], Rafael García de Sola[1] and Jesús Pastor[2]

[1]Neurosurgery and [2]Clinical Neurophysiology Services, Hospital Universitario de la Princesa, Diego de León 62, 28006, Madrid, Spain.

E-mail: gjortega.hlpr@salud.madrid.org

Abstract. Epilepsy is commonly associated with synchronous activity in the form of spikes and also in developed seizures. Desynchronised activity seems to play an important role also in the seizure process, favouring the initiation of seizures. The aim of the present work is to explore synchronization activity in the inner areas in the temporal lobe of epileptic patients by a novel approach. Two temporal lobe epilepsy (TLE) patients' records have been analyzed through a cluster analysis. Electrical activity in the inner part of the temporal has been recorded by using Foramen Ovale Electrodes (FOE), a semi-invasive technique frequently used in drug resistant epileptic patients. Instead of tracking synchronized activity, we give here special attention to desynchronized activity, mainly those areas which are not included in synchronization clusters. Our results show that electrical activity in the epileptic side behaves in a less cohesive fashion than the contra-lateral side. There exists a clear tendency in the epileptic side to be organized as isolated clusters of electrical activity as compared with the contra-lateral side, which is organized in the form of large clusters of synchronous activity. In particular, we shall give special attention to the cluster desynchronization during the seizures. As we shall show, our results can help in understand several characteristics of the seizures dynamics.

1. Introduction

Traditional methods used to assess correlated and synchronized activity in a system of interacting members has come to be revisited and generalized in recent years in order to cope with nonlinear and chaotic phenomena. In this sense new concepts, as for example weak, strong and generalized synchronization [1][2] are now widely used to describe the collective behavior of interacting systems and in particular, systems composed of neurons at several scales. More recently, the complex network theory [3][4] has provided new insights to approach the study of several kind of networks, in particular, brain networks, allowing to extract the main and distinctive properties of large assemblies of interacting neurons. In particular, detection of community structures [5][6] allows classify and organize different degrees of synchronized activity in a very comprehensible way.

Neural dynamics nowadays is an active field covered from several different points of views since the pure theoretical basis to the most clinical and practical perspective. Epilepsy, which traditionally have been associated to a synchronization disorder [7], or even more, with a hyper-synchronization disease [8][9], it is currently revisited and reinterpreted under the light of the new desynchronization point of view [10][11][12].

In the classical view [13][14] the epileptic activity in the form of epileptiform spikes displayed in the ElectroEncephaloGram (EEG) is caused by the hyper-synchronous activity in thousand of neurons

typically located in the hyppocampal and parahippocampal areas. This spiking activity remains confined to small regions, but sometimes, at the beginning of a seizure, the neurons' spiking activity overcome the surrounding inhibitions and then this synchronous activity begins to spread, activating synchronously large populations of neurons at distant areas [14], corresponding with the clinical manifestations of the epileptic seizures, commonly characterized as 'hypersynchronous states". Several works [9][10][11][12][15] however has apparently challenged this traditional view demonstrating that desynchronous activity is essential for the initiation and maintenance of epileptic seizures. Far from contradicting the classical knowledge, recent desynchronization results shed new light in the fragmented understanding we have today of the complex process which spark and sustain a developed and extended hypersynchronization activity during the clinical seizure. It is now fairly evident that in temporal lobe epilepsy (TLE) the whole process of seizure generation is associated with dramatic changes in neuronal synchronization at several, both temporal and spatial, scales mainly in the mesial region, amygdala, hippocampus and inner cortex of the brain, the major structures affected in this pathology.

In this paper we will introduce a new methodology to study synchronization activity in two TLE patients. Firstly, we will classify the community structures of the electrical activity in the inner side of the temporal lobe, recorded by FOE. We will identify desynchronized areas from the rest of the synchronization clusters by constructing a hierarchical tree of interactions, which we will call desynchronized electrodes (DE). We are able to identify the epileptic side, especially during the seizure by tracking the number of these DE along the entire FOE record. We will explain the proposed method in two TLE patients.

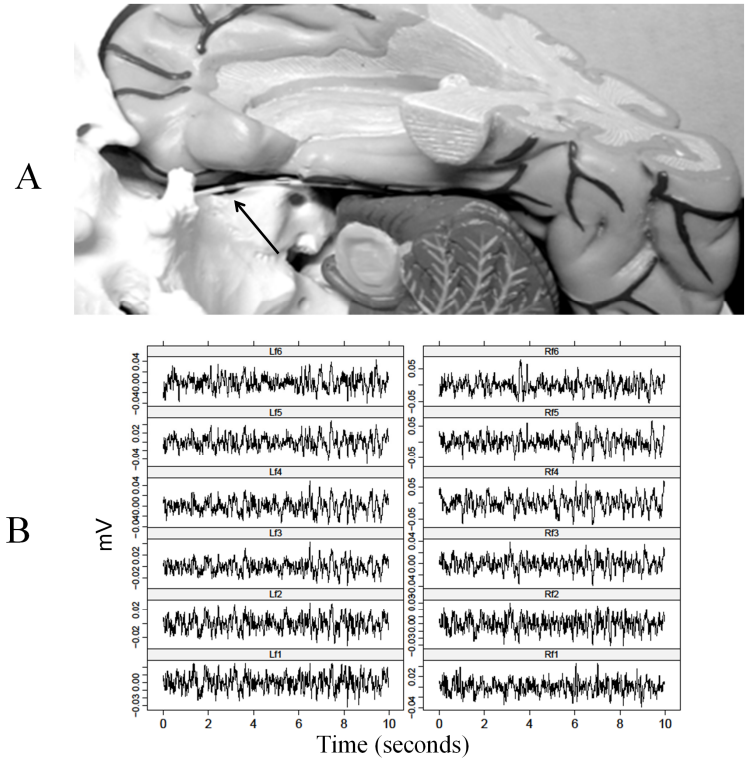

Figure 1: (A) Mesial aspect of the right temporal lobe and the right cerebellar hemisphere in a model of brain and skull. A foramen ovale electrode (FOE) was introduced through the right foramen ovale in order to demonstrate its localization within the mesial structures. The arrow indicate one of the six FOE locations. (B) Representative segments of FOE time series. Rf1-Rf6 stands for right FOE's #1 to #6 (right panel) and Lf1-Lf6 stands for left FOE's #1 to #6 (left panel).

Methods

1.1. Neurophysiological time series

Semi-invasive FOE technique has been developed [16] with the aim to record electrical activity at the inner part of the brain's temporal lobe, the main structure affected in temporal lobe epilepsy. Each FOE is a thin platinum wire, which is inserted through the ovale hole at the base of the skull. In this way, it allows to access deep structures in the head, especially the inner side of the brain, but without the need to go through into the brain. It records mainly the electrical activity at the surface of the inner side of the temporal lobe. Each wire consist of typically six contact electrodes [17] and during the placement procedure, two of these FOE are inserted bilaterally, one in each side of the brain. In figure 1 is displayed one FOE along its placement in between the inner part of the temporal lobe and other deep structures. The arrow in figure 1(A) shows one of the six electrodes in that FOE.

Digital FOE data, acquired at 500 Hz, filtered at 0.5–60 Hz and exported to ASCII format (XLTEK, Canada) at 200 Hz were used. Artifact free epochs lasting around 60 minutes were selected for further numerical analysis. All derivations were referenced to the scalp (Fz+Cz+Pz)/3 (standard 10-20 system). In figure 1(B) it is displayed ten seconds of a typical FOE record. Data were post-processed using Fortran and R programs. FOE will be named Lf1-Lf6 for the left electrodes and accordingly Rf1-Rf6 for the right electrodes.

Two neuro-physiological records have been analyzed in this work and both of them include a clinical seizure, characterized by a sudden change in the statistical properties of the electrical records which are translated in the typical epileptic symptoms. In figure 2 we show the standard deviation of all the scalp and FOE electrodes as a function of time. The clinical seizure onset, as indicated by the expert physician is around the minute 13.4. Clearly it can be seen the high and synchronous amplitude of several FOE, mainly in the left side. In this particular case, the patient suffers from a left TLE, which means that clinical seizures begin at this particular side of the temporal lobe, where the focus is supposedly located.

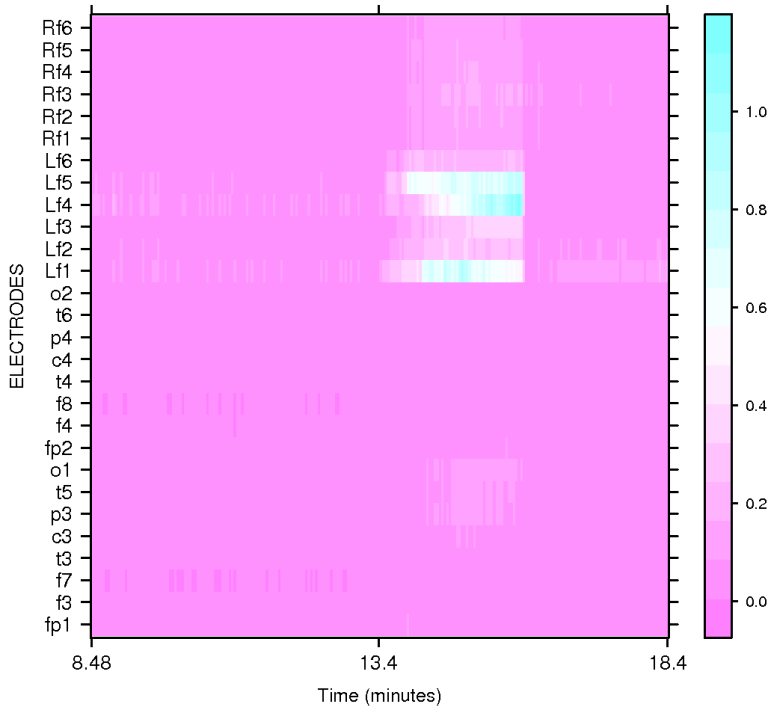

Figure 2: A typical neuro-physiological seizure of patient A. Level plot representation of the standard deviation in all electrical records, scalp and FOE. Clinical seizure begins at minute 13.4.

1.2. *Signal Analysis*

Multivariate FOE records of 12 channels (6 for each side) are divided in non-overlapping temporal windows of 512 data points (2.56 seconds). Longer values (1024 and 2048) have been used with qualitatively equivalent results. In each temporal window, cross-correlation among the 12 FOE time series was calculated, by using the Pearson correlation coefficient [18]:

$$\delta_{ij}(0) = \frac{\sum_{k=1}^{N_{win}} (x_i(k) - \overline{x_i})(x_j(k) - \overline{x_j})}{\sqrt{\sum_{k=1}^{N_{win}} (x_i(k) - \overline{x_i})^2 \sum_{k=1}^{N_{win}} (x_j(k) - \overline{x_j})^2}} \quad (1)$$

Where $\mathbf{x} = x_i(k), i = 1, N_{chan}$ *and* $k = 1, N_{win}$ is each of the 12 (N_{chan}) channels of 512 (N_{win}) data points each. We have selected this rather small number of points in each temporal window in order to obtain a suitable temporal resolution in each of the synchronization measures calculated (see below).

Correlation structure will be the base of our further calculations. No other synchronization measure will be used here. The main reason in using correlation instead of other nonlinear synchronization measures is that it performs well when it is used over neurophysiological data [10][18][19]. Another synchronization measure commonly used in recent years is phase synchronization [11][18], but as was very recently demonstrated, it must be used with extreme caution in neurophysiological electrical records [21].

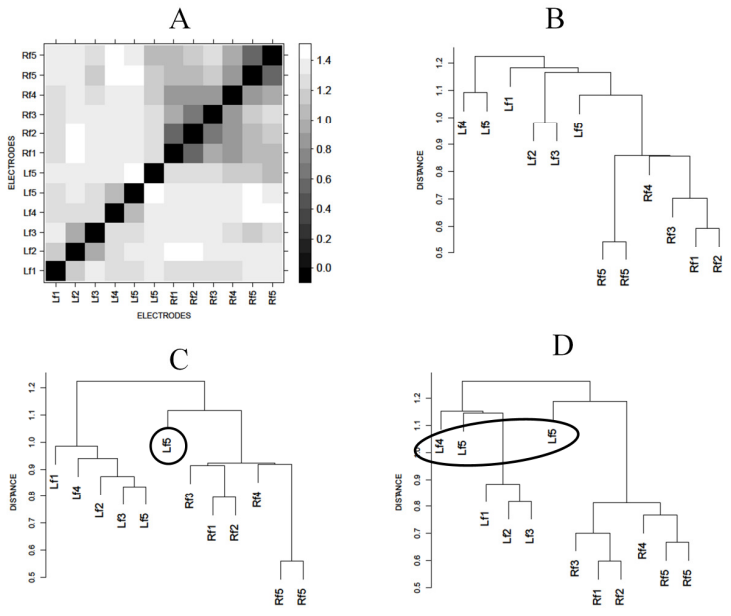

Figure 3: Synchronization and hierarchical trees. (A) Distance matrix for a particular temporal window of 512 data points in the patient A record. Only FOE electrodes are displayed. (B) Hierarchical tree (dendogram) corresponding to the distance matrix of (A). (C) and (D) two more dendogram corresponding to other temporal windows in the patient A record. Enclosed electrodes are DE (see text).

1.3. Community detection and desynchronized electrodes

In order to characterize the principal cortical interaction in the mesial area of the temporal lobe, we have implemented a recently developed algorithm aimed to detect clusters of interaction in a hierarchical tree, as it is for example the dendogram. The practical importance of hierarchical trees is that the data are not partitioned in a single step, but instead, a series of partitions are performed sequentially, accordingly with a specific rule. This is the best approach when there is no evidence in advance of how the interactions are organized. The hierarchical organization so obtained by any hierarchical clustering algorithm can be easily transformed in a community structure by simply *cutting* the hierarchical tree at a specific level.

In order to construct a distance organization from the interactions information, we shall transform correlation, as given by (1), in distances, in accordance with:

$$\rho_{ij} = |\delta_{ij}| \;\; ; \;\; d(i,j) = \sqrt{\rho_{ii} + \rho_{jj} - 2\rho_{ij}} = \sqrt{2(1-\rho_{ij})} \tag{2}$$

In this way, from the correlation matrix (1) we obtain the corresponding distance matrix. In figure 3 (A) we display a typical distance matrix for one of the temporal windows. From the distance matrix, it is now fairly easy to construct a hierarchical tree by using one of the traditional methods. We have chosen the agglomerative single-linkage [4] clustering technique. In this way, from the distance matrix, a hierarchical organization is achieved. In figure 3(B) it can be seen the dendogram corresponding to the distance matrix of figure 3(A). The correspondence between both figures is simply observed. In Figure 3(A) there exist higher correlations among the FOE of the right side than the correlations among the FOE of the left side, as displayed by the darker squares in the right side (upper-right corner), meaning shortest distances between the right electrodes. This fact is reflected in the dendogram, figure 3(B), where the right FOE are located at a deeper position in the tree that the left FOE, which are linked among them, but in an elevated position. We also display in figure 3(C) and 3(D) dendograms corresponding to other temporal windows. In these figures it is apparent that there exist equivalent correlations between the left and right electrodes, with the exception of few cases. Although both groups of electrodes are at the same level that is, left and right electrodes are grouped in individual clusters with similar height, there exists, however, some electrodes that appear outside the corresponding cluster. For instance, in figure 3(C) the left electrode Lf5 (encircled) appears desynchronized from the rest of the left electrodes because its high position in the dendogram. In the same way, left electrodes Lf4, Lf5 and Lf6 (enclosed) seems to be desynchronized from the synchronized cluster Lf1-Lf2-Lf3. These facts seem to favor the idea that there exists different cluster or community organization between both sides. Because the patient suffers from a left TLE, it seems that the areas covered by the left electrodes are less synchronized than the areas in the opposite side. In this way, we will give special attention to this kind of desynchronization.

1.4. Correlation measures

From the correlation matrix (1) we shall calculate three synchronization measures in order to compare against our results. All the calculated measures are normalized to its mean and standard deviation, for easy of comparison.

- Minimum Spanning Tree Cost (MSTC)
  From the correlation matrix it is possible to construct a tree, without loops, and with minimum total length in such a way that it represents the main interactions among the electrodes. This is called the Minimum Spanning Tree (MST). The total length of all the branches of the tree it is called "cost" of the MST. There exist a very simple way to construct the MST by using the Kruskal's algorithm. We shall use the MST cost as an

indicator of the seizure appearance because during a seizure exists an overall hyper-synchronization among different and distant areas in the brain, and in this way, the total cost of the MST must be reduced. We shall calculate the MST cost of all the FOE plus the scalp electrodes in order to consider the global synchronization produced during a clinical seizure.

- Average Synchronization (AS)
  In order to quantify the degree of synchronization among the FOE in each side, we shall simply sum the distances between pairs of FOE, for the left and for the right sides, and divide by two these quantities (due to the symmetric character of the distance matrix):

$$AS_{left} = \frac{1}{2} \sum_{i=1}^{6} \sum_{j=1}^{6} d(i,j) \quad and \quad AS_{right} = \frac{1}{2} \sum_{i=7}^{12} \sum_{j=7}^{12} d(i,j) \tag{3}$$

- Correlation eigenvalues (CE)
  Because the distribution of correlation eigenvalues (λi) is tightly linked to the synchronization characteristics of the time series, where a very unequal distribution of eigenvalues (for instance only one eigenvalue different from zero) implies a high synchronization among the time series, we shall calculate the following measure:

$$CE_{left} = \sum_{i=1}^{6} \lambda_i \log_2 \lambda_i \quad and \quad CE_{right} = \sum_{i=7}^{12} \lambda_i \log_2 \lambda_i \tag{4}$$

  When all the eigenvalues λi are equal, that is, all the time series are desynchronized we shall get a maximum of CE. On the other side, for a perfect case when exists only one eigenvalue different from zero, the case of a perfect synchronization, we shall get the minimum of CE. In this way, lower values of CE, either left or right, will mark the presence of synchronization among the involved electrodes. Note that correlation matrix must be definite positive for the proper (4) calculation. Any departure from this condition however must be due certainly produce by wrong inputs into the correlation matrix.

3. Results

We have applied the above described methods in two FOE records during typical patients' seizures. In each temporal window of 512 data points, we have calculated the correlation matrix through (1) and then transformed it into a distance matrix through (2). After that, a dendogram is constructed as explained in the Methods' section, and the identification of those electrodes that cannot be assigned to a synchronization cluster are counted. For instance, in figure 3(C) there is one electrode, namely Lf5 which seems to be desynchronized from the rest of all electrodes. Therefore, we count in this temporal window that there exists one left electrode that is not synchronized, or declusterized from the rest. In figure 3(D) instead, there exists three of these electrodes, Lf4, Lf5 and Lf6 which are declusterized because the three electrodes in the left side, Lf1, Lf2 and Lf3 seem to be tightly connected among them because its lower position in the dendogram. therefore we count 3 left DE in this temporal window. In the same way, all of the right FOE seems to be also strongly connected forming a large synchronized cluster of six electrodes.

In order to dig further into this fact we have implemented an automatic procedure to identify clusters of synchronous activity in every temporal window in records of approximately 60 minutes, yielding typically 360 temporal windows. To automatically detect synchronization clusters, we have selected a recently published algorithm [22] aimed to identify clusters in hierarchical structures as the

one depicted in figure 2. Given a minimum number of electrodes the clusters must have, the algorithm automatically extract and identify all of the clusters contained in the dendogram. Those remaining electrodes not belonging to any clusters continues unassigned and are labeled as DE.

In figure 4 we show the main results in the two selected records, A and B. In each case the results are divided in both left and right counts. For instance, in figure 4(A) we show the counts of DE for the left side (upper panel) and the counts of DE for the right side (lower panel). The solid vertical line marks the beginning of the seizure as indicated by the expert physician. It is remarkable the big difference between the number of DE in the left side as compared with the right side, where there exists more DE in the left side. In this sense, this temporal lobe displays lower synchronization than the right temporal lobe because the higher number of desynchronized electrodes in this side. Also, it is interesting to note the seizure synchronization effect around minute 13.4, where the seizure begins. The left side, where it is suspected that the focus resides, seems to be "unaware" of the synchronization wave produced by the seizure, contrary to what happens in the opposite side, the right one, where the few desynchronized electrodes are still present until the moment of the seizure onset, vanish almost instantaneously. It seems that during the seizure there exist a perfect synchronization in the right side and no appreciable effect in the left one. After 2 minutes of seizure however, it seems that there exists a higher level of synchronization in the left side, looking through the less number of DE in that side, and equal level of synchronization in the right side. It must bearing in mind that this patient suffers from a left TLE, that is, the origin of its seizures is in the left temporal lobe.

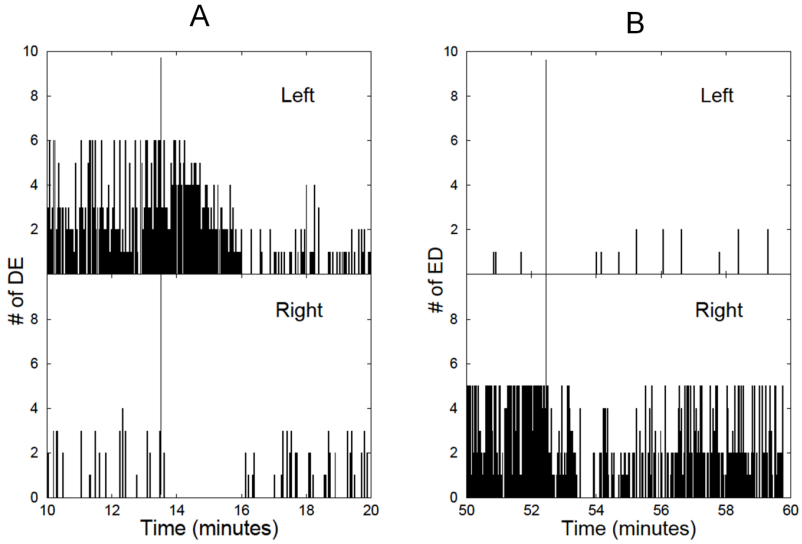

Figure 4: Number of DE as a function of time. (A) Both left and right DE counts as a function of time for patient A. (B) Both left and right DE counts as a function of time for patient B.

Something similar happens in the other patient's record, which suffers from a right TLE. The seizure onset is around minute 52.5. Also in this case, there exists a clear imbalance between right and left DE, being much more DE in the right side. After the seizure onset, it seems that there exists a lowering in the DE in the right, or epileptic, side, and none DE in the other side. But after a while after the seizure, it seems that the same levels of DE are achieved in both sides.

In order to compare our results against more classical measures, we display in figure 5 the calculations of the measures explained in the Methods section. In both cases, A and B of figure 5, we show the three measures. The seizure onset is marked by a vertical line. In the upper panel it is displayed the MST cost. In the middle panel we show the AS, for the left and right side, and in the lower panel the CE, also for the left and right sides.

The MST cost, which is a global synchronization measure, clearly shows a drop off at the beginning of the seizure, indicating that due to the higher level of correlations among all of the electrodes, the distances among them are reduced drastically.

AS are displayed in the middle panel of figure 5 (A) and (B). The solid line shows the AS_{left} and the dotted line the AS_{right}. In this case, there exists a striking difference between both sides because the left side shows a steepest drop off than the right side, at least during the seizure development, which finish when the seizure ends, approximately 2.5 minutes after the seizure onset. This effect is more intense in the patient A than in the patient B, either in intensity and in extent. The decrease in AS_{right} confirm the findings of figure 5 (A) because in the right side there exist a higher synchronization, expressed by the vanishingly number of DE as in figure 4 (A) and also by the lower values that the AS_{right} takes. Note that in the left side, there is a short period, just after the seizure onset, where the number of DE is higher than before the seizure onset (figure 4 (A)). This fact is confirmed by the short increase in the average distance in the left side in the middle panel of figure 5 (A).

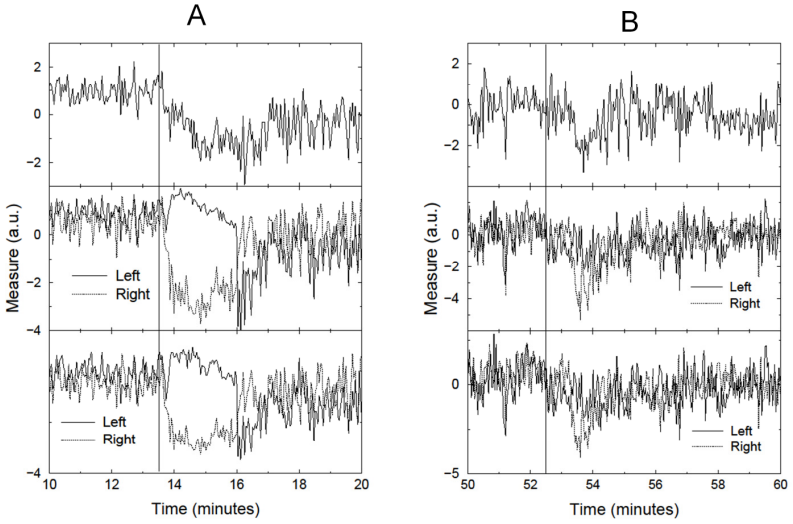

Figure 5: Correlation measures for both patients during the clinical seizure, as a function of time (10 minutes). All the measures are normalized to its mean and standard deviation. (A) Patient A, Upper panel: MST cost. Middle panel: AS for the left and right lobes. Lower panel: CE for the left and right lobes. (B). The same as in (A) but for patient (B).

Lastly, in the lower panel of figure 5 (A) and (B) we reproduce the calculations for the eigenvalues of the correlations matrix. By comparing these figures against the corresponding to the case of average synchronization, we can conclude that both measures behave in a very similar fashion.

4. Discussion

A clear imbalance between both mesial areas in TLE patients regarding its synchronization activity was shown here. Synchronization patterns have been quantified here by the property of being part of a synchronization cluster or not. Those areas belonging to any cluster have therefore its activity well synchronized with other areas within the cluster. In contrast, those regions which are not member of any cluster are, therefore, desynchronized from the rest, *i.e.* they are desclusterized regions. In both TLE patients shown here the area covered by the FOE's in the epileptic side behaves highly desclusterized as compared with the contra-lateral side, where mesial sites have a tendency to behave highly synchronized among them within one or several clusters. As we have also shown, declusterization is directly related with desynchronization in the whole side. The higher levels of declusterization displayed in the epileptic side produce lower levels of synchronization, as quantified by the synchronization measures used, AS and CE. Regarding these measures, both behaves in a

similar fashion, and also are easily calculated from the information provided by the FOE records. Thus, they can be used in analyzing large amount of data.

One of the main concerns in epileptology, especially in patients reluctant to drug treatment, it is the exact location of the focus, the supposedly origin of the clinical seizures because the last alternative treatment it is the surgical removal of the brain tissue responsible of the clinical symptoms. Although there is a vast battery of diagnostic techniques, as for example Magnetic Resonance Imaging, Single Photon Emission Tomography, Positron Emission Tomography and neurophysiological EEG signal, which are aimed at localize the true position of the epileptic focus, not always they accomplish its mission. In fact, in several occasions they yield contradictory results [23], for example, locating the epileptogenic area in different hemispheres. Although v-EEG is still the most confident lateralization and localization method, it largely relies in the analysis of the ictal phase as the true indicator of the seizure origin. Because of that, patients often remain in the v-EEG room for several days in order to account for a number of seizures which allow lateralize the epileptic side in a confidently way. The methodology described here seems to give more robust results with only two or three hours of analysis, saving therefore patients's time of hospitalization.

As we have shown in this paper, tracking the number of DE in each temporal lobe seems to be a reliable technique which allows easily and quickly get insight into the synchronization phenomena in the epileptic brain during the seizure, allowing the identification of the epileptogenic side.

Acknowledgments
We would like to thanks the LAWNP 2009 organizers, Celia Anteneodo and Marcos G.E. da Luz for their very kind hospitality during the conference. This work has been funded by grants from the Fundación Mutua Madrileña (GJO, JP) and from the Plan Nacional de Investigación Científica, Desarrollo e Innovación Tecnológica (I+D+I), Instituto de Salud Carlos III, PI060349 (JP, GJO, RGS). IHP is a predoctoral investigator from the Biomedical Research Foundation, Hospital Universitario La Princesa, Universidad Autonoma de Madrid. GJO is a member of CONICET.

References

[1] Schiff SJ, So P, Chang T, Burke RE andSauer T 1996 *Phys. Rev.* E **54(6)** 6708-24.
[2] Rulkov NF, Sushchik MM, Tsimring LS and Abarbanel HDI 1995*Phys. Rev.* E **51** 980-94.
[3] Albert R and Barabási AL 2002 *Rev. Mod. Phys.* **74** 47-97.
[4] Boccaletti S, Latora V, Moreno Y, Chavez M and Hwang D 2006 *Phys. Rep.* **424(4-5)** 175-308.
[5] Wasserman S and Faust K 1994 *Social Networks Analysis* (Cambridge University Press, Cambridge).
[6] Scott J 2000 *Social Network Analysis: A Handbook 2nd ed* (Sage Publications, London).
[7] Traub RD and Wong RK 1982 *Science* **216** 4547-745.
[8] Penfield W and Jasper H 1954 *Hypersynchrony. Epilepsy and the functional anatomy of the human brain* (Boston: Little, Brown and Company) pp 193-4.
[9] Schindler K, Leung H, Elger CE and Lehnertz K. 2007 *Brain* **130** 65-77.
[10] Netoff TI and Schiff SJ 2002 *J. Neurosci.* **22** 7297-307.
[11] Mormann F, Kreuz T, Andrzejak RG, David P, Lehnertz K and Elger CE 2003 *Epilepsy Res.* **53(3)** 173-85.
[12] Gutkin BS, Lang CR, Colby CL, Chow CC and Ermentrout GB 2001 *J. Comput. Neurosci.* **11** 121-34.
[13] Dichter MA and Ayala GF 1987 *Science* **237** 157-64.
[14] Kandel ER, Schwartz JH and Jessell TM 2000 *Principles of Neural Science 4th Edition* (McGraw-Hill, New York).
[15] Li Y, Fleming IN, Colpan ME and Mogul DJ 2008 *IEEE T. Neur. Sys. Reh.* **16(1)** 62-73.
[16] Wieser HG, Elger CE and Stodieck SR 1985 *Electroencephalogr. Clin. Neurophysiol.* **61(4)** 314–22.

[17] Pastor J, Sola RG, Hernando-Requejo V, Navarrete EG and Pulido P 2008 *Epilepsia* **49(3)** 464-9.
[18] Press WH, Teukolsky SA, Vetterling WT and Flannery BP 2003 *Numerical Recipes in Fortran 77 2nd Edition: The Art of Scientific computing*. (Cambridge University Press, Cambridge).
[19] Quian Quiroga R, Kraskov A, Kreuz T and Grassberger G 2002 *Phys. Rev.* E **65** 041903.
[20] Ortega GJ, Menéndez de la Prida L, García de Sola R and Pastor J 2008 *Epilepsia* **49(2)** 269-80.
[21] Guevara R, Velazquez JL, Nenadovic V, Wennberg R , Senjanovic G and Dominguez LG 2005 *Neuroinformatics* **3** 301-14.
[22] Langfelder P, Zhang B and Horvath S 2008 *Bioinformatics* **24(5)** 719-720.
[23] Pastor J, Hernando-Requejo V, Domínguez-Gadea L, de Llano I, Meilán-Paz ML, Martínez-Chacón JL, García Sola R 2005 *Revista de Neurología* **41(12)** 709-716.